Rev.Adv.Mater.Sci. 12 (2006) 33-45

# CRYSTAL GROWTH AND GIANT MAGNETORESISTANCE OF RARE EARTH LAYERED COBALTITES

**S. N. Barilo[1], S.V. Shiryaev[1], G.L. Bychkov[1], A.S. Shestak[1], Z.X. Zhou[2], V. Hinkov[3], V.P. Plakhty[4], Yu. P. Chernenkov[4], S.V. Gavrilov[4], M. Baran[5], R. Szymczak[5], D. Sheptyakov[6] and H. Szymczak[5]**

[1]Institute of Solid State and Semiconductor Physics, BAS, 17 P. Brovka st., Minsk 220072, Belarus
[2]National High Magnetic Field Laboratory, 18 E. Paul Dirac Dr., Tallahassee, FL 32310, USA
[3]Max-Planck Institut für Festkörperforschung, 1 Heisenberg str., D-70569 Stuttgart, Germany
[4]Petersburg Nuclear Physics Institute, 188300 Gatchina, Russia
[5]Institute of Physics, Polish Academy of Sciences, Al. Lotników 32/46, PL-02 668 Warsaw, Poland
[6]Laboratory for Neutron Scattering, ETH Zürich & Paul Scherrer Institute, CH-5232, Villigen PSI, Switzerland

*Received: November 12, 2005*

**Abstract.** A review on progress in crystal growth and study of layered cobaltites is presented. Single crystals of the $LnBaCo_2O_{5+\delta}$ (Ln = Pr, Sm, Eu, Gd, Tb, Dy, $Tb_{0.9}Dy_{0.1}$) family with the giant magnetoresistance (MR) effect were grown by the flux technique. Co-crystallization with the geometrically frustrated $LnBaCo_4O_7$ phase was registered in a wide range of temperature. The details of structure of the as-grown and detwinned single crystals and their characterization by magnetic susceptibility, magnetoresistance, X-ray and neutron diffraction are discussed. A comparative study of the twinned and twins free $EuBaCo_2O_{5+\delta}$ single crystals reveals a positive magnetoresistance effect ~ 500% at low temperature.

## 1. INTRODUCTION

It was unambiguously shown that fascinating properties of cobaltites can be tuned by chemical engineering to allow the observation of a spin-gap formation in the geometrically frustrated *Kagomé* lattice of the cobalt layers [1], the highly anisotropic giant magnetoresistance (MR) effect in a specific temperature range [2,3] and uncommon superconductivity [4]. There are direct evidences that *Ba*-doped cobaltites $LnBaCo_2O_{5+\delta}$ (Ln – rare earth or yttrium, $0 \le \delta \le 1$) undergo spin, charge and orbital ordering when the oxygen content approaches $\delta$ = 0.50. Here exotic magnetic properties resulting in the highest amongst cobalt based oxides value of MR and a metal-insulator transition on the verge of $Co^{3+}$ spin state transition may be manifested, and often unusual valence states of cobalt are maintained. Taking in mind that $Co^{2+}$, $Co^{3+}$, and $Co^{4+}$ ions are all susceptible to become apparent in multiple spin states one can consider the $LnBaCo_2O_{5+\delta}$ (Ln-112, $0 \le \delta \le 1$) family as a model system to investigate most of the possible electronic configurations of cobalt. In particular, for the nominal valence of cobalt 3+ at $\delta$ = 0.5 the $Co^{3+}$ ion has a non-magnetic, or low-spin ground state (LS, $t_{2g}^6 e_g^0$) as well as the intermediate-spin (IS, $t_{2g}^5 e_g^1$) and the high-spin (HS, $t_{2g}^4 e_g^2$) excited states.

The Ln-112 phase at $\delta$=0.5 has orthorhombic structure with the unit cell $a_1 \approx a_p$, $a_2 \approx 2a_p$, $a_3 \approx 2a_p$, where $a_p$ is parameter of the pseudocubic perovskite cell, which is usually described by the *Pmmm* space

Corresponding author: S.N. Barilo, e-mail: bars@ifttp.bas-net.by

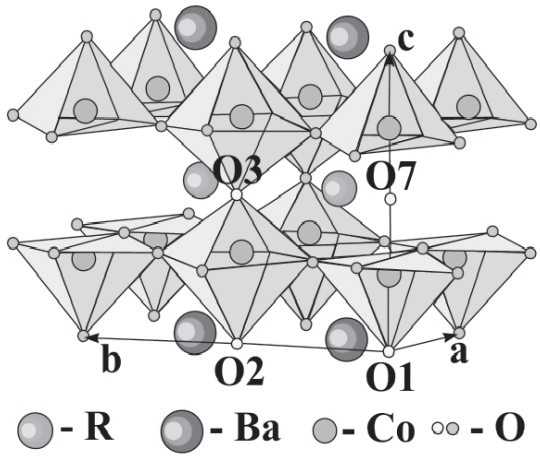


**Fig. 1.** Unit cell of the layered perovskite $LnBaCo_2O_{5.5}$. Open small circles show the crystallographic positions, which can be partially occupied by the $O^{2-}$ ions.

group [5-8]. As shown in Fig. 1, the structure represents a sequence of stacking plains $[CoO_2][BaO][CoO_2][LnO_\delta]$ along c-axis, which results in the two types of cobalt environment: $CoO_5$ square pyramids and $CoO_6$ octahedra. This oxygen ordering occurs in the Ln-112 family at $\delta \approx 0.5$, where oxygen ions demonstrate alternating filled and empty chains in $LnO_\delta$ plains, causing a tetragonal to orthorhombic transition and doubling of the unit cell along the *b*-axis. Usually, such a transition is accompanied by development of a highly twinned structure of crystals that mixes the *a* and *b* orthorhombic axes. As in the case of a well-known superconductor $YBa_2Cu_3O_{7-x}$, one needs to perform a detwinning procedure to obtain a single domain orthorhombic crystal [3].

The change of spin configuration is one of the remarkable phenomena characteristic of the Ln-112 family of cobalt oxides. A review of controversial publications, mainly concerning $TbBaCo_2O_{5+x}$ ($\delta \sim 0.5$) [9-11], demonstrates that the $Co^{3+}$ spin ordering in these materials, which one could expect to be independent on the rare earth, at least in the high-temperature range, is still unknown. In case of $TbBaCo_2O_{5.5}$, the identical magnetic structures were established for two ceramic samples differing by conditions of preparation [12]. One of them had a single 'main' magnetic and crystal phase whereas the second sample had two crystal phases and, as a consequence of partial oxygen disorder, a more sophisticated magnetic phase, in fact, consisting of the 'main' and 'erroneous' ones.

Based on resistivity studies of precisely oxygenated powder and singly crystals of Gd-112 ($0 \le \delta \le 0.77$), it was shown [13] the layered cobaltite never becomes a true metal over a wide range of oxygen variation from 0.5 electrons per Co ($\delta = 0$) to 0.27 holes per Co ($\delta = 0.77$). Despite never being a normal metal the Ln-112 resistivity does not behaves either as a simple insulator or semiconductor, but as temperature increases above ~ 250K the in-plane resistivity $\rho_{ab}(T)$ exhibits either a gradual crossover or a sharp transition into a metal-like state with a high enough value $\rho_{ab} \sim 500$ $\mu\Omega\cdot$cm on the metal side of the metal insulator (MI) transition. One can also mention an intriguing feature of Gd-112 when in contrast to the samples ($\delta > 0.50$), which reveal rather conventional resistivity evolution with the hole doping, upon reducing $\delta$ below 0.50 (electron doping) an initial decrease of the resistivity suddenly turns into a resistivity growth. This fact, in line with the observed insensitivity of the absolute value of resistivity and its temperature dependence to doping over a wide range $\delta \le 0.44$, distinguish these compounds from both conventional band and Mott insulators. Such a situation may only be possible if the released electrons upon removing oxygen do not participate in the charge transport. This assumption is in an excellent agreement with the results of thermoelectric measurements in the oxygen deficient Ho-112 compound [14]. The authors concluded that below the MI transition insulating behavior results from the $Co^{3+}$ spin state transition to a low-spin state of $Co^{3+}$ sited in the octahedra. In this case the transport occurs at the expense of hopping of the low-spin $Co^{4+}t_{2g}$ holes, whereas the high-spin $Co^{2+}$ electrons are captured due to a so called spin blockade.

The MR anisotropy studies with respect to direction of the applied field can provide deep information on the cobalt-spin anisotropy. Recent experimental studies of Ln-112 (Ln = Gd, Eu) showed that the MR anisotropy is surprisingly large [13,15,16]. The large negative MR of detwinned Eu-112 was measured to be associated with the orbital ordering of $t_{2g}$ states in $Co^{3+}$ caused by a strong spin-orbital coupling [16]. Moreover, it was shown that magnitude and even sign of the MR effect could be varied with oxygen doping and temperature [15,16].

Large and high quality single crystals are essential to provide thorough neutron scattering studies as well as synchrotron and other spectroscopic

**Table 1.** Comparison: cuprates versus cobaltites from the point of crystal growth from an overstoichiometric flux melt based on use of alumina crucibles.

| $LnBa_2Cu_3O_{7-x}$ (HTSC layered cuprate) | $LnBaCu_2O_{5+\delta}$ (layered cobaltite) |
|---|---|
| Incongruent melting | Incongruent melting |
| Higher solubility | Lower solubility |
| Lower growth temperature (1010 – 950 °C) | Higher growth temperature (1300 – 1150 °C) |
| Narrow primary crystallization field | Narrow primary crystallization field |
| Lower flux creep | Higher flux creep |
| Higher flux corrosivity | Lower flux corrosivity |
| Lower flux melt viscosity | Higher flux melt viscosity |
| Co-crystallization: | Co-crystallization: |
| $Ba_{1-y}Ln_yCuO_2$ (y ~ 2-3 at.%) | $LnBaCu_4O_{7+\delta}$; $Ba_{1-x}Ln_xCo_{1-y}Al_yO_{3-z}$ |

investigations of electronic and spin structure. However, due to difficulties of growth, until now there have not been much data published on Ln-112 single crystals. One can refer to a few reports on successful measurements of the single crystals (Ln = Pr, Nd, Sm, Gd, Tb) grown by the floating zone (FZ) method [11,13,17-19]. However, most details of growth are omitted in these papers, which do not allow comparing advantages and disadvantages of the FZ approach to grow single crystals in this essentially incongruent melted system. One can mention only a rather slow growth rate of 0.5 mm/hr, which has been used to reduce a number of domains in the multidomain crystal rode. Single crystals with the perfectly ordered Gd-112 crystal structure were obtained by this FZ process [13]. We suppose that advantages of the traveling solvent floating zone technique has been recently used to grow successfully a large Nd-112 single crystal [20].

Expanded fields of full melting in the range 1200 – 1280 °C were recently found in the corresponding $Ln_2O_3$ - BaO - CoO Gibbs triangles [15,16]. Using these data single crystals of Ln-112 (Ln = Pr, Eu, Gd, Tb, Dy) with rectangular shape and dimensions up to $5\times7\times0.5$ mm$^3$ have been successfully grown from overstoichiometric flux melts to reveal uncommon magnetic and magnetoresistance behavior [21-23]. However, caused by features of nucleation and a significant flux melt creep and a significant corrosion of alumina crucibles, single crystals of Ln-112 (Ln = Nd, Sm, Ho or Y) have not yet been grown by the flux technique. A comparison of growth features of the well-known superconductors $LnBa_2Cu_3O_{7-x}$ and Ln-112 layered cobaltites is shown in Table1. Both the families possess common thermodynamics and growth features, namely, incongruent melting, very narrow the primary crystallization fields (PCF) and co-crystallization with other complex phases, which provide serious difficulties in growth of large crystals. However, a lower solubility of Ln-112 (up to 3 mass %) and consequently a higher (~1300 – 1150 °C) growth temperature create additional problems in crystal growth of this phase. In order to overcome these problems we have comprehensively studied the binary eutectic point (~1115 °C) and its composition in the BaO – CoO system . Moreover, investigations of the Ln-112 phase PCFs in the corresponding quasi-ternary phase diagrams have been recently undertaken [22-24].

Usually, the Ln-112 single crystals grown by the FZ method and then thermally treated in the flowing oxygen to a proper oxygen content show all magnetic reflections [11], which have been observed for very different oxygen contents ($\delta < 0.5$) [25]. This and the data recently obtained on the precisely characterized Gd-112 single crystals [13] present an indication that the crystal structure and a value of the MR effect are very sensitive to oxygen. In particular, to its distribution over possible crystallographic sites and to the sample homogeneity at some average oxygen content. It was also clearly demonstrated by the recent investigations of structural and mag-

netic properties of Pr-112 ($0.16 < \delta < 0.90$) [26-28]. The magnetic properties confirm an extreme sensitivity of the $\delta \sim 0.5$ region to the sample preparation method. In particular, while for $\delta < 0.35$ an antiferromagnetic state is found to be independent on the cooling rate, compounds with oxygen stoichiometry close to $\delta \sim 0.50$ display magnetization curves which depend strongly upon the synthesis history. The data presented [13,26] are incontestable evidence that a special attention should be paid to systematic control and characterizing of oxygen distribution in the layered cobalt perovskites. Otherwise erroneous conclusions about the magnetic properties (as well as spin state of Co) could be reached.

In this review paper, we report some of the PCF data as well as our not yet very successful attempts to get limited nucleation and successive growth of Ln-112 (Ln = Y, La, Nd, Sm, Ho). For most of the $Ln_2O_3$ - BaO - CoO systems co-crystallization with a new geometrically frustrated magnetic phase $LnBaCo_4O_{7+\delta}$ (Ln-114) [1] was recently found [22,23]. Then we will concentrate on application of recently developed approaches to flux growth [24] and advantages of use MgO crucibles to provide limitation of a nuclei number and to grow large and high quality single crystals of the Ln-112 family. Characterization of both families by magnetic properties and X-ray diffraction will be done. We will also discuss a highly anisotropic behavior of magnetic susceptibility and metamagnetic transitions between magnetically ordered phases both in the cobalt and terbium sub-lattices of the detwinned single crystal $Tb_{0.9}Dy_{0.1}BaCo_2O_{5.5}$. A comparative study of the MR properties in Eu-112 single crystals grown by two different approaches of the flux melt technique is presented.

## 2. EXPERIMENTAL PROCEDURE

Furnaces with a vertical chamber supplied by Cr-La resistive heaters were used to grow single crystals of the Ln-112 (Ln = Pr, Sm, Eu, Gd, Tb, Dy) and Ln-114 (Ln = Eu – Yb and Y) phases by the flux melt technique. Either spontaneous crystallization or growth of a limited number of nuclei at almost constant temperature under positive temperature gradient of 1-3 °C over a crucible height were used. Temperature controllers RIF –101 (Ukraine) were used to provide an accuracy of temperature stabilization of ± 0.1 degree at homogenization temperature up to 1320 °C and rates of supercooling of the flux melt in the range 0.05–10 °C/day. More than 100 crystallization runs were done in the Co-enriched parts of the corresponding Gibbs triangles. We used to prepare the flux melts by direct melting of initial powder components to grow the cobaltates. One can follow the details of the procedure, which have been already described [23,24]. In addition, the recently developed approach of flux growth and MgO crucibles were used to initiate nucleation and provide large and high quality single crystals of some compounds. Briefly, a batch of rare earth oxide was put as feeder on the bottom of a 100 $cm^3$ magnesia crucible to keep the overstoichiometric flux melt saturated at ~ 1200 °C under a few degrees of positive temperature gradient for about three weeks of isothermal crystal growth process. The mixture of high purity $BaCO_3$ and $Co_3O_4$ in the ratio 2BaO – 3CoO was used as solvent. As a result, in successful growth runs, several crystals of a parallelepiped shape with exceptionally clean and shinny faces were found on a special shape magnesia crystal holder, which was kept slowly rotated during the whole growth run. There is no efficient solvent to extract Ba-doped cobaltite crystals from the solidified fluxes. That is why we used to mechanically evoke them after 10 hrs of soaking by porous bricks at about 1130 °C. The structures of the Ln-112 and Ln-114 phases were determined with a four cycle X-ray diffractometer, PNPI Gatchina, the Siemens D500 X-ray diffractometer and HRPT diffractometer at SINQ, PSI Villigen with neutron wavelength 1.494 Å. All as-grown Ln-112 crystals except Pr-112 (this compound needs in reduction of oxygen) were annealed for 20 hrs at 600 °C and 3 bars of oxygen pressure. Then isobaric cooling down to RT with rate of 10°C/hr was used. Iodometric titration provided a sampling estimation of oxygen content to be $\delta = 0.50 \pm 0.02$. The oxygenated and twinned Ln-112 single crystals were cut along the crystal axes and polished. A piece of gold foil was attached to each of two opposite faces of the sample where uniaxial pressure is applied along the *a*(*b*)-axis. Two different regimes were used to get twinned and twins free Eu-112 samples (Table 2): (a) the crystals were kept for 10-20 hrs in flowing oxygen at 300-350 °C and then quickly cooled to room temperature under pressure of about 0.15-0.2 GPa; (b) some of the samples were heated to 400 °C in ambient atmosphere and then cooled slowly to room temperature under pressure of ~ 0.15 GPa. The twinned crystal structure of the optimally oxidized ($\delta = 0.5$) orthorhombic crystals as well as quality of the above detwinning procedure were characterized using a polarized-light optical microscope.

The grown Ln-112 and Ln-114 crystals were characterized by DC susceptibility in the temperature

**Table 2.** Conditions of growth and detwinning of the $EuBaCu_2O_{5+\delta}$ single crystals.

| Sample | Temperature range and cooling rate growth | annealing | Environment |
|---|---|---|---|
| Eu-112 – I (as-grown) | ~1190 °C (positive temperature gradient ~ 3-5 °C) | 600 °C-RT (10 °C/hr) | Air 3 bar, oxygen |
| Eu-112 – I (detwinned) | | ~300 °C | Flowing oxygen |
| Eu-112 - II (as-grown) | 1350-1000 °C (2 °C/hr) | | Air |
| | | 1000 °C -RT (80 °C/hr) | Air |
| Eu-112 – II (detwinned) | | 400°C-RT (10 °C/hr) | Air |

range 2 – 300K and an external field up to 9 and 5 T using QUANTUM design system PPMS-9 and SQUID magnetometer MPMS-5, respectively. Measurements of magnetization were carried out with a commercial SQUID magnetometer (Quantum Design, MPMS-5) in a temperature range 2 - 380K in magnetic fields up to 5 T. The external magnetic field was applied along all crystal axes and, in a particular case, along the <110> and <101> directions. Sometimes the thermomagnetic history of measured samples was taken into account, so the measurements were carried out in the zero field cooling mode (ZFC) as well as in field cooling with measurements on cooling (FCC) and on warming (FCW) modes.

A vibrational sample magnetometer was used to measure isothermal magnetization up to 33 T at the NHMFL in Tallahassee. Resistivity and magnetoresistance were measured using a standard four probe technique. Gold contacts were sputtered onto the samples to reduce contact resistance.

## 3. RESULTS AND DISCUSSION

### 3.1. Initial nucleation and growth of the Ln-112 and Ln-114 phases

Typical conditions of nucleation and results of more than 100 runs of the Ln-112 and Ln-114 crystals growth either in alumina or in magnesia crusibles are summarized in Table 3. High quality single crystals of Ln-112 (Ln = Pr, Eu, Gd, Tb, Dy) with rectangular shape and dimensions up to 7x5x1mm$^3$ were successfully grown under spontaneous crystallization conditions. After successful growth runs, which were done for one or three weeks either in alumina or magnesia crucibles under optimized conditions of initial nucleation, several a parallelepiped shape crystals of Ln-112 (Ln = Sm, Eu, Gd, Dy, $Tb_{0.9}Dy_{0.1}$) and up to 150 mm$^3$ in volume were found on the surface of a drawn out crystal holder. However, in spite of a variety of parameters have been used to reach nucleation, such as material of the crystal holder, its shape and temperature as well as stirring rate and a value of temperature gradient in the flux melt, we have not yet been succeeded in nucleation of the Ln-112 phase with Y, La, Nd, and Ho. Unfortunately, it was not possible neither to generate nucleation, nor to get a number of nuclei limited for the listed compounds under ambient conditions because of a significant creep and a high viscosity (in the case when alumina crucibles were used) and perhaps other physical and chemical features of the flux melts.

Fortunately, co-crystallization of the Ln-112 and Ln-114 phases was observed in a wide range of compositions and temperature for most the $Ln_2O_3$ - BaO – CoO systems. Bulk and good quality Ln-114 (Eu – Yb and Y) single crystals of hexagonal prismatic shape up to 300 mm$^3$ in volume were grown (Fig. 2).

**Table 3.** The main crystallizing phases depending on rare earth oxide concentration in the $LnO_{1.5}$-$Ba_2Co_3O_y$ cross section of corresponding Gibbs triangles and a crucible material.

| Rare earth oxide | Rare earth ionic radius, nm | Number of growth runs | Initial growth temperature, $T_{sc}$, °C or cooling range | $Ln_2O_3$ molar number in flux | Main crystallizing phase |
|---|---|---|---|---|---|
| | | | **Alumina crucible** | | |
| $Pr_2O_3$ | 0.100 | 13 | 1312 - 1295 | 0.4 - 0.25 | 112 |
| $Nd_2O_3$ | 0.099 | 2 | 1156; 1213 | 0.2; 0.5 | P |
| $Sm_2O_3$ | 0.097 | 1 | 1193 – 1156 | 0.2 | 112; P |
| | | 2 | 1250 - 1226 | 0.3 | 112 |
| $Eu_2O_3$ | 0.097 | 4 | 1262; 1231 | 0.25 | 114 |
| | | | 1238; 1243 | 0.3 | 112 |
| $Eu_2O_3$/$Gd_2O_3$ | | 5 | 1204; 1221; 1229 | 0.194/0.006 | 112 |
| $Gd_2O_3$ | 0.094 | 27 | 1250; 1260 | 0.116-1.0 | 112, 114 |
| | | | 1230 -1159 | 0.13 | P |
| $Tb_2O_3$ | 0.089 | 44 | 1297 – 1154 | 1.0 | 114 |
| | | | | 0.25 | 114; 112 |
| | | | | 0.2 | 114; 112; P |
| | | | | 0.15 | p |
| $Dy_2O_3$ | 0.088 | 21 | 1252-1210 | 0.5 – 0.2 | 112; 114; P |
| | | | 1200 - 1191 | | |
| $Ho_2O_3$ | 0.086 | 16 | 1295 - 1217 | 0.15-1.0 | 114; P |
| | | | | 0.13 | P |
| $Y_2O_3$ | 0.097 | 6 | 1204; 1229 | 0.4 | 114 |
| | | | 1205 – 1219 | 0.2 | 114 |
| | | | 1153 - 1141 | 0.1 | P |
| $Er_2O_3$ | 0.085 | 1 | 1340-1220 | 0.25 | 114 |
| $Tm_2O_3$ | 0.085 | 1 | 1287-1204 | 0.25 | 114 |
| $Yb_2O_3$ | 0.081 | 1 | 1340-1220 | 0.25 | 114 |
| $Tb_2O_3$/$Dy_2O_3$ | | 17 | 1205 - 1191 | 0.18/0.02 | 112; 114 |
| $Pr_2O_3$/$Dy_2O_3$ | | 1 | 1197 - 1167 | 0.1/0.1 | P; 112 |
| $Tb_2O_3$/$Y_2O_3$ | | 1 | 1188 - 1158 | 0.18/0.02 | 114; P |
| | | | **Magnesia crucible** | | |
| $Gd_2O_3$ | 0.094 | 3 | 1200 | 0.2 | P |
| | | | 1208-1205 | 0.2 | 112 |
| | | | 1237-1221 | 0.2 | 112 |
| $Eu_2O_3$ | 0.097 | 6 | 1229-1213 | 0.3 | P;112 |
| | | | | 0.3 | 112 |
| $Dy_2O_3$ | 0.088 | 2 | 1229-1217 | 0.24 | P;112 |
| | | | 1237-1217 | 0.24 | 112 |
| $Tb_2O_3$ | 0.089 | 3 | 1200-1186 | 0.2 | CoO |
| | | | 1246-1222 | 0.2 | CoO |
| | | | 1287-1227 | 0.2 | P, CoO |

The powder X-ray and neutron diffraction patterns were indexed in the hexagonal unit cell for this compound with parameters *a*=6.29795 Å, *c*=10.22481 Å. A solution of the structure has been found in the space group $P6_3mc$ [1]. As shown in Fig. 3, this Ln-114 structure has also a layered character, but in

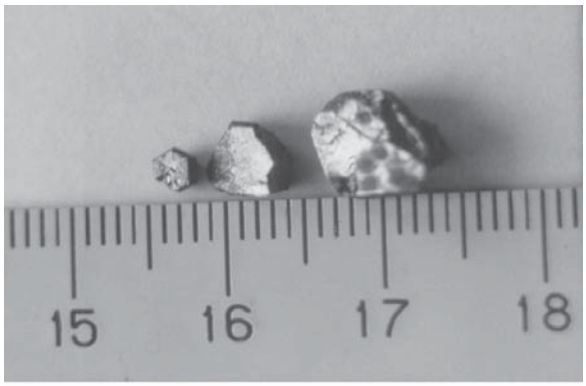


**Fig. 2**. As-grown single crystals of $HoBaCo_4O_{7+\delta}$.

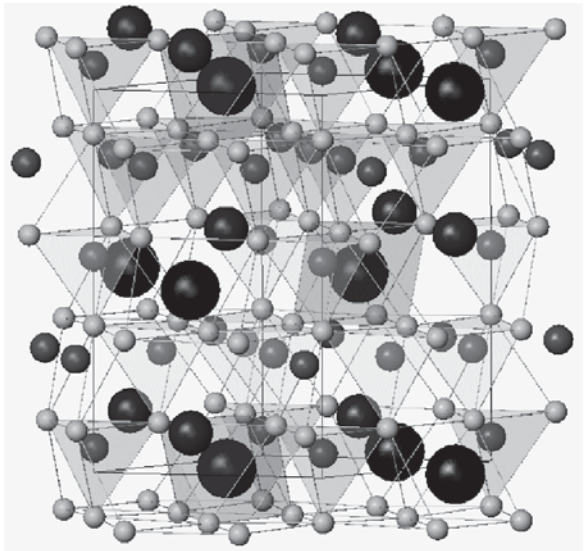

**Fig. 3.** Hexagonal crystal structure of the layered $HoBaCo_4O_{7+\delta}$: Ho (big blacks); Ba (medium blacks); Co (small blacks); O (small grays). Unit cellis marked by solid line.

contrast to the Ln-112 phase, one of the layers is formed by repeated sequence of three $CoO_4$ tetrahedra, while another one contains one $CoO_4$ tetrahedron and one $HoO_6$ octahedron, the vast cavity in this layer being filled by the 10-fold coordinated Ba cation. All these polyhedra are being interconnected via their corners. This structure represents an example of a Kagomé net with the geometrical spin frustration, when one consider only the cobalt ions.

## 3.2. Nuclei formation and primary crystallization fields of the layered cobaltates

The PCFs, for the case when alumina crucibles and crystals holders have been used, are presented in

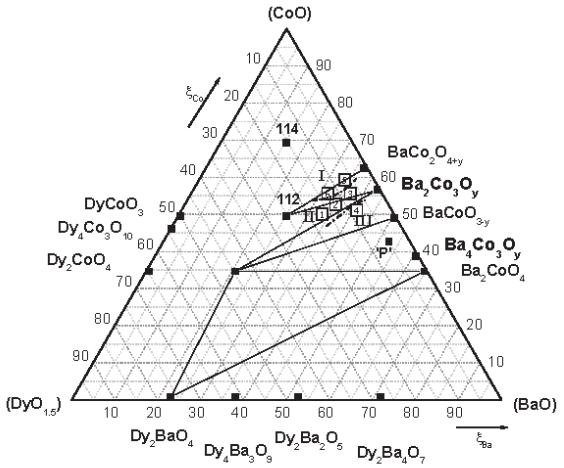


**Fig. 4.** Primary crystallization fields of co-crystallized cobaltate phases in the Co-enriched part of the $Dy_2O_3$ – BaO – CoO quasi-ternary phase diagram.

Fig. 4 for the cobaltate phases, which appear in a part of the Dy-Ba-Co-O quasi-ternary phase diagram in air. Among others, reliable and reproducible experimental data were obtained only in the Gd-, Eu- and Dy-based phase diagrams; they confirm a stable range of Ln-112 phase primary crystallization in the whole temperature interval 1100-1300 °C. In Range II of compositions, black colour single crystals of this phase were used to nucleate and grow over the whole volume of crucible; these crystals mainly have a shape of thin rectangular plates. When the concentration of Co and Dy oxides increases, a transition to the PCF of Dy-114 (Range I) occurs, while a considerable decrease of Dy content and steady state lowering of the CoO/BaO ratio in the flux cause the double perovskite Dy-112 and perovskite ('P') $Ba_{1-x}Dy_xCo_{1-y}Al_yO_{3-z}$ phases to co-crystallise and a gradual transition into the primary crystallization range (III) of the perovskite phase [23]. Based on preliminary results of the recenly done growth experiments with use crucibles and holders from magnesia, one can expect a more narrow PCFs both for the Ln-112 and for Ln-114 phases to exist, and a significant shift to appear of both the ranges to a higher rare earth content. In the other quasi-ternary systems differing in rare earths except Sm one can detect either lack of nucleation or much narrower ranges of temperature and the flux compositions,

where nuclei of Ln-112 phase were registered on the surface of crystal holder. Unfortunately, neither variation of the crystal holder material and shape nor its compulsory cooling were much of help to create a limited number nuclei and to grow Ln-112 (Ln = Nd, Tb, Ho) single crystals under temperature gradient. It is still not quite undestood why the PCFs of the Ln-112 phase seem to become smaller in accordance with the series Gd, Eu, Dy, Tb, Sm, Pr, Nd and to disapear completely for Ho and apparently for Y in the same temperature range. Last two systems revealed the Co-enriched Ln-114 as the main phase, which crystallizes in air. In fact, for flux compositions in the intervals $Ho_2O_3$ (3.85-14.93 mol.%), BaO (36.6-40.3 mol.%), CoO (44.8-57.7 mol.%), stable crystallization of the Ho-114 phase was obtained, while until now we have neither successful crystal growth nor nucleation of the Ho-112 phase. In turn, for Dy- and Tb-based systems, co-crystallization of all above mentioned cobaltate phases was registered in most growth runs due to instability of flux composition caused by the flux melt creep and alumina crucibles corrosion. These problems are a much smaller obstacle in nucleation of the Ln-112 phase for the case when magnesia crucibles and holders are used.

Fortunately, the task of large size crystal growth has been successfully solved, when ~10% of $Dy_2O_3$ has been added to the terbium oxide feeder at the bottom of crucible. Indeed, stable growth conditions and a much more stable (and limited) initial nucleation were found for the $Tb_{0.9}Dy_{0.1}$–112 phase. However, the reason of this is still unclear and additional growth experiments, which have been already undertaken on the other mixed rare earth cobaltites were not successful.

### 3.3. Distribution of oxygen atoms in the $Tb_{0.9}Dy_{0.1}$–112 single crystals

The most reliable information on the degree of oxygen ordering among the apical positions, which is responsible for the formation of octahedral and pyramidal Co-sites in Ln-112 can be obtained from a neutron diffraction experiment. Before a polarized neutron diffraction experiment planned for a twinned crystal of $Tb_{0.9}Dy_{0.1}$-112 to distinguish the spin density distribution in octahedra and pyramids, intensity 269 nuclear reflections have been measured to refine the crystal structure. The results of the crystal structure refinement are shown in Table 4. One may recognize a pyramid with O1 at (0,0,0) with some traces of oxygen in the position of vacancy at (0,0,z) as shown in Fig. 1. The positions of O2, O3 are not filled completely by oxygen, which means that octahedra and pyramids are distributed almost statistically at $y$ = 1/2 and there are some traces of oxygen in the position O7 (see Fig. 1). The number of oxygen atoms for the formula unit is 4.71(2) instead of 5.5. The experiment has demonstrated that the ordering of pyramids and octahedra is very poor here, and it should be treated once more. However, high radioactivity of cobalt nuclei after neutron irradiation makes this impossible. Even for this crystal, there was an indication of difference in spin density distribution between the layers at $y$ =0 and $y$ = 1/2. Note that one has to have a detwinned crystal and well ordered octahedra and pyramids to investigate spin density of $Co^{3+}$ ion and $O^{2-}$ ligand in both sites (not only the difference between octahedra and pyramids), which is very important for understanding the properties of these materials.

To solve the second task, we have developed an X-ray diffraction method to control the perfection of oxygen ordering in the unit cell between subsequent crystal treatments. First, we have calculated the intensity dependence on oxygen content in O1, O2, O3, and O7 sites for a number of X-ray reflections measured in reflecting geometry with Ag-K$\alpha$ radiation. It penetrates in the crystal for about 0.15 mm, and the characteristics obtained should be valid for all the crystal with a thickness of ~0.5 mm. With reflection (0,2,14) used as a standard, the occupation of these positions by oxygen can be determined with a precision good enough for our purpose. In spite of low sensitivity of the method to the light oxygen atom on the background of heavy Tb, Ba, and Co atoms, distribution of oxygen over its apical positions in a large detwinned single crystal $Tb_{0.9}Dy_{0.1}BaCo_2O_{5.5}$ was controlled by X-ray diffraction with a precision of 0.01–0.02. As it was recently shown for $GdBaCo_2O_{5.5}$ and $DyBaCo_2O_{5.5}$ [29], there is unambiguous evidence that the symmetry changes from Pmmm in paramagnetic phase to Pmma at the MI transition. Terbium is placed between Gd and Dy in the periodic table and it is quite natural to expect that $Tb_{0.9}Dy_{0.1}BaCo_2O_{5.5}$ possesses the same Pmma symmetry at room temperature. The integrated intensities of 93 independent reflections were measured; 87 of them were used in the crystal structure refinement in the frame of space group Pmma. At the beginning of the least squares refinement, the parameters of the unit cell, the atomic coordinates, and their isotropic temperature factors were taken for $TbBaCo_2O_{5.5}$ from Ref. [12]. All necessary corrections of the intensity have been made, for absorption, polarization, and Lorentz-

**Table 4.** The results of the structure refinement of a not optimally oxygenated $Tb_{0.9}Dy_{0.1}BaCo_2O_{5.21(3)}$ single crystal based on 269 nuclear reflections. The refinement quality is given by $\chi^2 = 7.3$; $R_{wp} = 0.095$.

| Atom | Site | *x* | *y* | *z* | Content |
|---|---|---|---|---|---|
| Tb | 2*p* | 1/2 | 0.2670(5) | 1/2 | 0.890(5) |
| Dy | 2*p* | 1/2 | 0.2670(5) | 1/2 | 0.110(5) |
| Ba | 2*o* | 1/2 | 0.2477(9) | | 1.00(1) |
| Co1 | 2*r* | 0 | 1/2 | 0.2515(16) | 1 |
| Co2 | 2*q* | 0 | 0 | 0.2526(16) | 1 |
| O1 | 1*a* | 0 | 0 | 0 | 1.000(18) |
| O2 | 1*e* | 0 | 1/2 | 0 | 0.516(9) |
| O3 | 1*g* | 0 | 1/2 | 1/2 | 0.816(17) |
| O4 | 2*s* | 1/2 | 0 | 0.3086(7) | 1 |
| O5 | 2*t* | 1/2 | 1/2 | 0.2824(8) | 1 |
| O6 | 4*u* | 0 | 0.2427(6) | 0.2968(4) | 1 |
| O7 | 1*c* | 0 | 0 | 1/2 | 0.083(19) |

**Table 5.** Atomic coordinates $x/a_1$, $y/a_2$, $z/a_3$, isotropic temperature factors *B*, and occupancies *n* determined for the detwinned $Tb_{0.9}Dy_{0.1}BaCo_2O_{5.5}$ single crystal at room temperature. The crystal symmetry is orthorhombic (*Pmma*; $Z = 4$), and the lattice parameters are $a_1 = 7.74$ Å, $a_2 = 7.80$ Å, $a_3 = 7.55$ Å. The refinement quality is given by $\chi^2 = 3.1$; $R_{wp} = 4.2$.

| Atom | Position | $x/a_1$ | $y/a_2$ | $z/a_3$ | *B* | *n* |
|---|---|---|---|---|---|---|
| Tb(Dy) | 4*h* | 0 | 0.2730(2) | 0.5 | 0.38(1) | 1 |
| Ba | 4*g* | 0 | 0.2494(2) | 0 | 0.45(1) | 1 |
| CoPy1 | 2*e* | 0.25 | 0 | 0.2522(3) | 0.17(1) | 1 |
| CoPy2 | 2*e* | 0.25 | 0 | 0.7388(4) | 0.17(1) | 1 |
| CoOc1 | 2*f* | 0.25 | 0.5 | 0.2488(5) | 0.17(1) | 1 |
| CoOc2 | 2*f* | 0.25 | 0.5 | 0.7444(6) | 0.17(1) | 1 |
| O1 | 2*e* | 0.25 | 0 | 0.0000(6) | 0.75(3) | 1.00(1) |
| O7 | 2*e* | 0.25 | 0 | 0.5 | 0.75(3) | 0.09(2) |
| O2 | 2*f* | 0.25 | 0.5 | -0.0048(6) | 0.75(3) | 1.00(2) |
| O3 | 2*f* | 0.25 | 0.5 | 0.50(1) | 0.75(3) | 1.00(1) |
| O4 | 4*i* | 0.023(2) | 0 | 0.391(1) | 0.75(3) | 1 |
| O5 | 4*j* | 0.0019(4) | 0.5 | 0.2710(7) | 0.75(3) | 1 |
| O61 | 4*k* | 0.25 | 0.249(3) | 0.289(2) | 0.75(3) | 1 |
| O62 | 4*k* | 0.25 | 0.294(5) | 0.666(2) | 0.75(3) | 1 |
| Twins | | | | | | 0.91(2) |

factor. The extinction correction [30] has been found insignificant. In addition to the apical oxygen occupancies, all other parameters were refined, namely, coordinates of cobalt atoms in pyramidal (CoPy1, CoPy2) and octahedral (CoOc1, CoOc2) sites, of the oxygen atoms (O1 – O62), as well as the twin population, see Table 5. The averaged oxygen content is 5.54(2) and the twin population 0.91(2). The resolution of a four-circle diffractometer is not good enough to observe directly the twins, but the difference of *a* and *b* has been detected by reflections from corresponding crystal edges. We are planning to use this or similar single crystal of $Tb_{0.9}Dy_{0.1}$-112 in a polarized neutron diffraction experiment in the

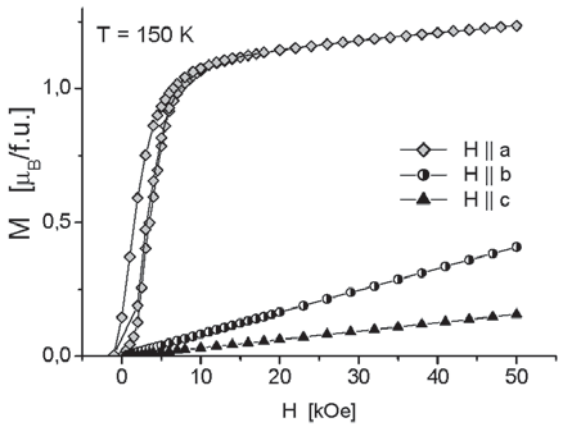


**Fig. 5**. Isothermal magnetization at $T$ = 150K of the detwinned $EuBaCo_2O_{5.48}$ single crystal (Sample Eu-112-I) in the external magnetic field oriented parallel to the main crystallographic axes.

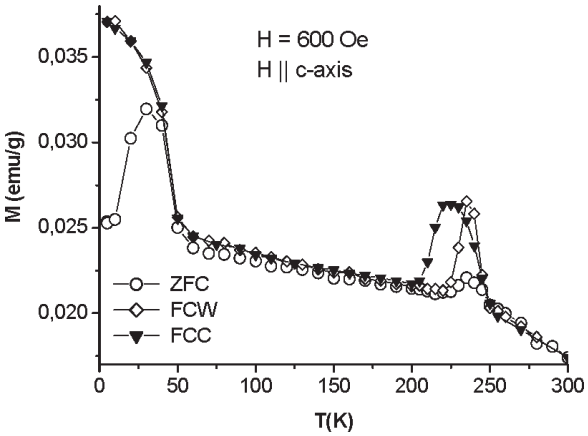


**Fig. 6.** DC magnetization versus temperature for the detwinned $EuBaCo_2O_{5.48}$ (Sample Eu-112-I) in $H$ = 600 Oe; $H$ || $c$-axis for three regimes: zero field cooling (ZFC), field cooling with measurements on cooling (FCC) and on warming (FCW).

nearest future with the aim to establish the magnetic moment distribution over the cobalt ions $Co^{3+}$ and ligands in both pyramidal and octahedral sites.

## 3.4. Magnetization and magnetoresistance of the twins free Ln-112 single crystals

Magnetization of the detwinned $Tb_{0.9}Dy_{0.1}$-112 single crystal has been recently studied [31]. The admixture of Dy has no essential influence on behavior of the rare earth subsystem of this compound, which is determined by the single ion anisotropy of terbium. Indeed, the $Tb^{3+}$ sub-system in the antiferromagnetic (AFM) range ($T < T_{N2}$ = 3.4K) is strongly anisotropic with easy axes [101] and [$10\bar{1}$]. It is also shown that $Co^{3+}$ ions are of the Ising type with the easy axis along the $a$ axis, in the temperature range 2 – 276K. At low temperature, magnetic field induced phase transitions were studied to show that they are determined by anisotropic exchange interactions $Co^{3+}$- $Tb^{3+}$. It is obvious the $Co^{3+}$ subsystem is ferrimagnetically (FM) ordered within the range $T_N<T<T_C$ ($T_N$=250K, $T_C$=276K) and the FM→AFM phase transition is of the first order, whereas the phase transition from FM to paramagnetic (PM) state is of the second order. In the region of AFM ordering of $Co^{3+}$ ions, the metamagnetic phase transition were observed for $H$ || $a$ (Fig. 5). A small ferromagnetic component along the $a$ axis has been also seen in the temperature range 2 < $T$ < 170K.

A comparative study of the MR effect was done on the Eu-112 crystals (Samples I and II), which have been grown from an overstoichiometric flux melt and post growth treated either by different approaches (Table 2). According to the huge anisotropy observed in the magnetization data for the both types of Eu-112 crystals, the twins within the $ab$ plane were largely removed (Fig. 6). Temperatures of the PM→FM→AFM transitions for Sample II are higher than the corresponding temperatures for the Eu-112-I crystal [16,32]. However, the magnitude of the peak $M(T)$ for $H$ || $a$ in Sample I is much larger than in Sample II and all twinned crystals. There are two possible reasons for this: (1) the oxygen content in Sample II used in this study is closer to $\delta$ = 0.5 than in Sample I, so that an onset of long-range order may occur at a higher temperature, and, contrarily, (2) the magnetic domains are better aligned and larger in Sample I. At low temperatures (below $T \approx$ 50K), a spin-glass-like state [32,15], which gives a contribution to the difference between $M_{ZFC}$ and $M_{FC}$ and to a huge hysteresis for $H$ || $a$ which was registered for both samples (Fig. 7).

One can see (Fig. 8a) the giant positive MR of the twinned Eu-112-I single crystal with current flow and $H$ in the $ab$ plane, reaching 500% at $T$ = 40K

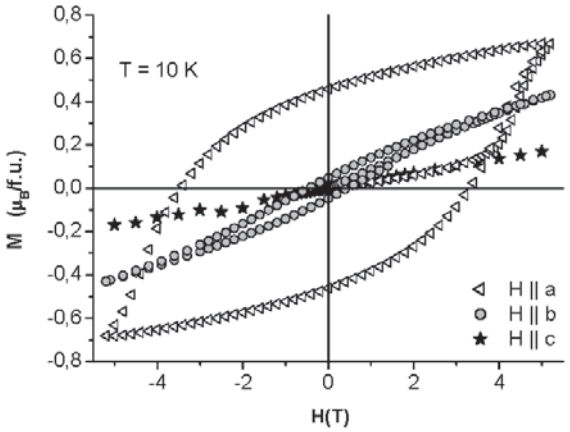


**Fig. 7.** *M*(*H*) dependences of Sample Eu-112-I (at 10K) for different magnetic field orientations.

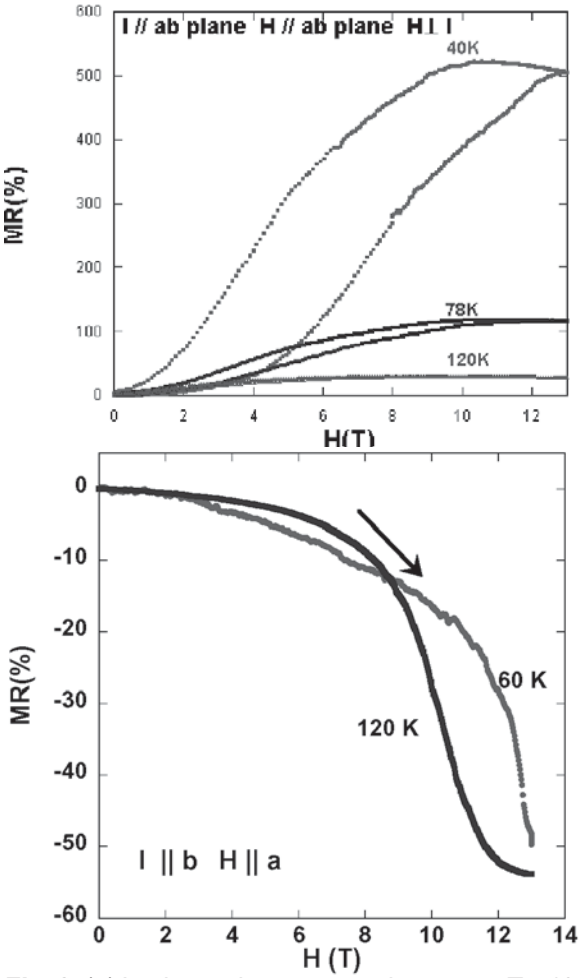


**Fig. 8.** (a) Isothermal magnetoresistance at $T = 40$, 78 and 120K of the twinned $EuBaCo_2O_{5.5}$ single crystal (Sample Eu-112-I; $I \perp c$-axis, $H \perp c$-axis, $H \perp I$); (b) Isothermal magnetoresistance at $T = 60$ and 120K of the twins free $EuBaCo_2O_{5.5}$ single crystal (Sample Eu-112-II; $I \parallel b$-axis; $H \parallel a$-axis).

and $H = 13$ T. The magnitude and hysteresis of MR in this case decrease with increasing temperature, and it changes sign to become negative at $T > 120$K. In contrast, coinciding with the metamagnetic transition, the isothermal resistivity of the detwinned Eu-112-II single crystal shows a steep decrease for current flow $I \parallel b$ and applied field $H \parallel a$ in the range $60 \leq T \leq 260$K, and negative MR as large as 53% at $T = 120$K and $H = 13$ T was measured (Fig. 8b.). For the $H \parallel a$ (easy axis), the negative MR is much more pronounced when the current flows along *c*-axis [16].

Similar to the cases of geometrically frustrated $Na_{0.75}CoO_2$, oxygen deficient metallic $VO_x$ films, and $La_{2/3}Ba_{1/3}MnO_3/LaNiO_3$ superlattices [33], we attribute the positive MR phenomenon to the presence a strong magnetic disorder on the verge of the AFM interlayer coupling in the Eu-112-I crystals caused by oxygen deficiency and a small mixing of Eu valence. Indeed, since $Eu^{3+}$ ions do not have a magnetic moment, the $M_{FC}(T)$ is essentially flat at low temperatures except for a small but noticeable broad shoulder both for $H \parallel a$ and $H \parallel b$, suggesting that long range AF order coexists with spin-glass-type behavior below 50K possibly due to inhomogeneous oxygenation. Another possible explanation is a weak valence admixture of the Eu-ions, which could have an intermediate valence close to but less than 3+.

The magnetic susceptibility of such disordered systems at low temperature may be strongly spatially inhomogeneous. Then, local parts of the crystals with higher AFM correlations rise in the external field, and, finally, the Ising type AFM ordering will develop to increase significantly charge localization.

In contrast to the Ln-112 case, no long range magnetic ordering was found in the Ho-114 single crystals until $T = 2$K. However, a significant diffuse scattering of neutrons was registered for the first time below $T = 15$K to show evidence of local spin-

spin antiferromagnetic correlations. A very high probability exists that the spin-singlet ground state will appear at very low temperatures in this geometrically frustrated Kagomé network. The electronic spin resonance and Raman measurements of these crystals are in progress and will be published elsewhere.

## 4. CONCLUSIONS

The initial nucleation of $LnBaCo_2O_{5+\delta}$ and $LnBaCo_4O_{7+\delta}$ (Ln = Nd – Yb) was studied in the range 1100–1300 °C for the flux melt compositions, which correspond to primary crystallization fields of the cobaltate phases. High quality single crystals of $LnBaCo_2O_{5+\delta}$ ($0 < \delta < 1$; Ln = Sm, Eu, Gd, $Tb_{0.9}Dy_{0.1}$) with rectangular shape and dimensions up to 150 $mm^3$ (as for the case $Tb_{0.9}Dy_{0.1}$-112) were grown using the technique of mass transfer to a limited number of nuclei at a few degrees of positive temperature gradient. Bulk single crystals of $HoBaCo_4O_7$ up to 300 $mm^3$ in volume were grown for the first time. They were used in studies of Ho crystal field excitations and cobalt spin-spin and spin-lattice relaxation rates by inelastic neutron scattering.

Highly anisotropic Ising-like magnetic behavior and huge anisotropy of the giant MR phenomenon are typical for single crystals of Ln – 112 (Ln = Eu, $Tb_{0.9}Dy_{0.1}$), while only short-range magnetic correlations were registered for their Co-enriched counterparts. Our results with use of twins free single crystals confirm a two sublattice magnetic structure of Ln – 112 in which the intermediate spin (S=1) $Co^{3+}$ ions are FM ordered within the planes of $CoO_5$ square pyramids. Coinciding with the threshold field of induced transition in magnetization, the isothermal resistivity of the twins free $EuBaCo_2O_{5.5}$ single crystal reveals a steep decrease for $H \parallel a$ axis demonstrating the giant negative MR. Surprisingly, for the twinned Eu-112 single crystal grown by another way, the MR at a low temperature with current flow in the *ab* plane, is positive reaching ~ 500%. The magnitude and hysteresis of MR in this case decrease with increasing temperature, and the MR changes sign and becomes negative at $T > 120$K. We attribute this phenomenon to strong magnetic disorder in the crystals at low temperatures caused by oxygen deficiency and slightly mixed valence of Eu.

## ACKNOWLEDGMENTS

Financial support by NATO in frame of Collaborative Linkage grant # PST CLG 979369, and by grants BRFFI-RFFI ## 04P-143, 04P-163 and BRFFI 05-129 (Belarus), KBN 1 PO3B 038 27 (Poland), the Russian Foundation for Basic Researches (Project 05-02-17466-a) and State Program 'Quantum Macrophysics' (grant SS-1671.2003.2) is gratefully acknowledged.

## REFERENCES

[1] D.V. Sheptyakov, A. Podlesnyak, S.N. Barilo *et al*., *PSI Scientific Report 2001 (ISSN 1423-7326, March 2002) v. III Cond. Mat. Research*, p. **64**; M. Valldor and M. Andersson // *Solid State Sciences* 4 (2002) 923.

[2] A. Maignan, C. Martin, D. Pelloquin, N. Nguen and B. Raveau // *J. Solid State Chem.* **142** (1999) 247.

[3] A. A. Taskin, A. N. Lavrov and Y. Ando // *Phys. Rev. Lett*. **90** (2003) 227201.

[4] K. Takada, H. Sakurai, E. Takayama-Muromachi, F. Izumi, R.A. Dilanian and T. Sasaki // *Nature* (London) **422** (2003) 53.

[5] M. Respaud, C. Frontera, J.L. García-Muńoz, M.A. G. Aranda, B. Raquet, J.M. Broto, H. Rakoto, M. Goiran, A. Llobet and J. Rodriguez-Carvajal // *Phys. Rev. B* **64** (2001) 214401.

[6] S. Roy, M. Khan, Y,Q. Guo, J. Craig and N. Ali // *Phys. Rev. B* **65** (2002) 064437.

[7] C. Frontera, J.L. García-Muńoz, A. Llobet and M.A.G. Aranda // *Phys. Rev. B* **65**, (2002) R180405.

[8] C. Frontera, J.L. García-Muńoz, A. Llobet, L.I. Macosa and M.A.G. Aranda // *J. Solid State Chem.* **171** (2003) 349.

[9] D.D. Khalyavin, I.O. Troyanchuk, N.V. Kasper, Q. Huang, J.W. Lynn and H. Szymczak // *J. Mater. Res.* **17** (2002) 838.

[10] F. Fauth, E. Suard, V. Caignaert and I. Mirebeau // *Phys. Rev. B* **66** (2002) 184421.

[11] M. Soda, Y. Yasui, T. Fujita, T. Miyashita, M. Sato and K. Kakurai // *J. Phys. Soc. Jpn* **72** (2003) 1729.

[12] V.P. Plakhty, Yu.P. Chernenkov, S. N. Barilo, A. Podlesnyak, E. Pomjakushina, E.V. Moskvin and S.V. Gavrilov // *Phys. Rev. B* **71** (2005) 214407.

[13] A.A. Taskin, A.N. Lavrov and Y. Ando // *Phys. Rev. B* **71** (2005) 134414.

[14] A. Maignan, V. Caignaert, B. Raveau, D. Khomskii and G. Zawatzky // *Phys. Rev. Lett.* **93** (2004) 026401

[15] Z.X. Zhou, S. McCall, C.S. Alexander, J.E. Crow, P. Schlottmann, S.N. Barilo, S.V.

Shiryaev and G.L Bychkov // *Phys. Rev. B* **70** (2004) 024425.
[16] Z.X. Zhou and P. Schlottmann // *Phys. Rev. B* **71** (2005) 174401.
[17] M. Soda, Y. Yasui, M. Sato and K. Kakurai // *J. Phys. Soc. Jpn.* **73** (2005) 1875.
[18] M. Soda, Y. Yasui, M. Ito S. Iikubo, M. Sato and K. Kakurai // *J. Phys. Soc. Jpn.* **73** (2004) 464.
[19] T. Sato, T. Arima, Y. Okimoto and Y. Tokura // *J. Phys. Soc. Jpn* **69** (2000) 3525.
[20] Yoichi Ando, private communication.
[21] D.D. Khalyavin, S.N. Barilo, S.V. Shiryaev, G.L. Bychkov, I.O. Troyanchuk, A. Furrer, P. Allenspach, H. Szymczak and R. Szymczak // *Phys. Rev. B* **67** (2003) 214421.
[22] G.L. Bychkov, S.V. Shiryaev, A.G. Soldatov, A.S. Shestak, S.N. Barilo, D.V. Sheptyakov, Conder, E. Pomjakushina, A. Podlesnyak, A. Furrer and R. Bruetsch // *Cryst. Res. Techn.* **40** (2005) 395.
[23] G.L. Bychkov, S.N. Barilo, S.V. Shiryaev, D.V. Sheptyakov, S.N. Ustinovich, A. Podlesnyak, M. Baran, R. Szymczak and A. Furrer // *J. Cryst. Growth* **275** (2005) 813.
[24] S.N. Barilo, S.V. Shiryaev, G.L. Bychkov, V.P. Plakhty, A.S. Shestak, A.G. Soldatov, A. Podlesnyak, K. Conder, M. Baran, W.R. Flavell and A. Furrer // *J. Cryst. Growth* **275** (2005) 120.
[25] D. Akahoshi and Y. Ueda // *J. Solid State Chem*. **156** (2001) 355.
[26] S. Streule, A. Podlesnyak, J. Mesot, M. Medarde, K. Conder, E. Pomjakushina, E. Mitberg and V. Kozhevnikov // *J. Phys.: Condens. Matter* **17** (2005) 3317.
[27] C. Frontera, J.L. García-Muńoz, A.E. Carrillo, C. Ritter, D. Martin, Y. Marero and A.Caneiro // *Phys. Rev.* **70** (2004) 184428.
[28] C. Frontera, J.L. García-Muńoz, A.E. Carrillo, A.Caneiro, C. Ritter and D. Martin Y Marero // *J. Appl. Phys*. **97** (2005) 10C106.
[29] Yu. P. Chernenkov, V. P. Plakhty, V. I. Fedorov, S. N. Barilo, S. V. Shiryaev and G. L. Bychkov // *Phys. Rev. B* **71** (2005) 184105.
[30] P. J. Becker and P. Coppens // *Acta Cryst. A* **30** (1974) 129.
[31] M. Baran, V.I. Gatalskaya, R. Szymczak, S.V. Shiryaev, S. N. Barilo, G. L. Bychkov and H. Szymczak // *J. Phys. Cond. Matter.* **17** (2005) 5613.
[32] M. Baran, S. N. Barilo, G. L. Bychkov, V.I. Gatalskaya, L.A, Kurochkin, S.V. Shiryaev, R. Szymczak and H. Szymczak // *Acta Physica Polonica A* **105** (2004) 209.
[33] In some cases, mostly in the layered structures one observes a positive MR, which is usually ascribed either to rise of an interlayer scattering with field, or to specific electronic structure and strong intrinsic magnetic disorder, see, e.g., R. Malik, E.V. Sampathkumaran and P.L. Paulose // *Appl. Phys. Lett.* **71** (1997) 2385; K.R. Nikolaev, A.Yu. Dobin, I.N. Krivorotov, W.K. Cooley, A. Bhattacharya, A.L. Kobrinskii, L.I. Glazman, R.M. Wentzovitch, E. Dan Dahlberg and A.M. Goldman // *Phys. Rev. Lett*. **85** (2000) 3728; A.D. Rata, V. Kataev, D.I. Khomskii and T. Hibma // *Phys. Rev. B* **68** (2003) 220403 (R); T. Motohashi, R. Uead, E. Naujalis, T. Tojo, I. Terasaki, T. Atake, N. Karppinen and H. Yamauchi // *Phys. Rev. B* **67** (2003) 064406.